Electromagnetic structure functions and neutrino nucleon scattering

M. H. Reno
Department of Physics and Astronomy, University of Iowa, Iowa City, Iowa 52242 USA

Electromagnetic structure functions for electron-proton scattering are used as a test of the QCD improved parton model at low and moderate Q^2. Two parameterizations which work well in ep scattering at low Q^2 are used to evaluate the inelastic muon neutrino-nucleon and muon antineutrino-nucleon cross sections for energies between 1-10 GeV, of interest in long baseline neutrino oscillation experiments. Cross sections are reduced when these low-Q^2 extrapolations are used.

I. INTRODUCTION

Neutrino physics has been a topic of considerable interest, especially since the discovery of neutrino oscillations [1] in the context of solar neutrinos [2] and atmospheric neutrinos [3]. Determinations of neutrino mass squared differences and mixing angles have led to long baseline neutrino experiments [4] where the energies of the neutrino beams range between a few hundred MeV to tens of GeV. In the few GeV region, it is a theoretical challenge to describe the neutrino-nucleon cross section with high precision [5]. Theoretical issues include the problem of making the transition between exclusive and inclusive calculations, and the fact that one is generally in a Q^2 regime where the coupling constant $\alpha_s(Q^2)$ is large.

Currently, experimental data in this kinematic region for neutrino scattering are sparse [6], although experiments are planned to remedy this situation [7, 8]. Theoretical work has started to address the issue of combining exclusive and inclusive processes in Ref. [9]. One element of the calculation is the deep inelastic scattering (DIS) contribution, which is the focus of this paper. We assess the perturbative QCD description of the electroweak structure functions in the kinematic regime relevant to the neutrino cross section at a few GeV incident energy. We do this by considering the electron-proton electromagnetic structure functions where there are extensive data [10]. The breakdown of the perturbative description occurs at a Q^2 scale of $Q^2 \sim 1$ GeV^2 when one compares electromagnetic scattering data with structure function calculations. In electromagnetic scattering, below ~ 1 GeV^2, phenomenological parameterizations can be used in place of the parton model based evaluations of the structure functions.

There are parameterizations of the structure functions over the full range of x and Q that successfully describe the electromagnetic data [11, 12], however, it is not completely obvious how to generalize these parameterizations to the neutrino scattering case. Bodek, Yang and Park [13, 14] have taken a different approach, namely to extract flavor components of structure functions even in the nonperturbative regime [15]. This is explicitly applicable to neutrino scattering. Here, we examine a structure function parameterization by Capella et al. [16, 17] which does well in electron-proton scattering at low values of Q^2 and at the same time has a straightforward transformation to neutrino charged current scattering. The parameterizations of Capella et al., and by Bodek, Yang and Park are described and compared below.

In the next section, we show the results of a perturbative evaluation of the DIS charged current cross section in the intermediate (few GeV to 10 GeV) energy range to establish which kinematic regions contribute most to the cross section. In Section III, we use ep scattering results to show the range of validity of perturbative QCD and the efficacy of the two phenomenological parameterizations of the structure functions into the non-perturbative regime. Section IV shows how the extrapolations translate to the structure functions relevant to neutrino scattering. Comparisons of the different approaches to low Q^2 structure functions in neutrino-nucleon charged current cross sections are shown in Sec. V.

II. DIS IN νN SCATTERING

Of particular interest is the neutrino cross section for energies up to 10-20 GeV. One approach [5] to the cross section in this energy regime is to add three separate contributions to the cross section: the (quasi)elastic weak scattering contribution which leaves the nucleon intact [18], the resonant contribution in which a finite number of resonances including the Δ are included [19], and the inelastic contribution to sum the remaining terms [20]. To avoid double counting, the evaluation of the inelastic piece is done over a restricted phase space. Generally, something like a limit on the hadronic final state invariant mass W, such $W^2 > W^2_{\rm min} \sim 2$ GeV^2, is applied. We use $W_{\rm min}$ to separate the exclusive and inclusive calculations, and we focus only on the inclusive portion of the cross section.

As Lipari, Lusignoli and Sartogo emphasized [5], the charged current cross section components for $\nu_\mu N$ scattering from quasi-elastic, Δ resonance production, and deep inelastic scattering (DIS) with $W^2 > 2$ GeV^2 are about equal for $E_\nu \sim 2$ GeV. The DIS term grows with increasing energy.

"Deep" inelastic scattering is a misnomer in this case because of the sensitivity to the cross section to low-Q^2. Neutrino-isoscalar nucleon scattering

$$\nu_\mu(k)\, N(p) \to \mu(k')\, X$$

is discussed in terms of $q = k - k'$, $Q^2 \equiv -q^2 \geq 0$, the invariant momentum transfer to the hadronic system,

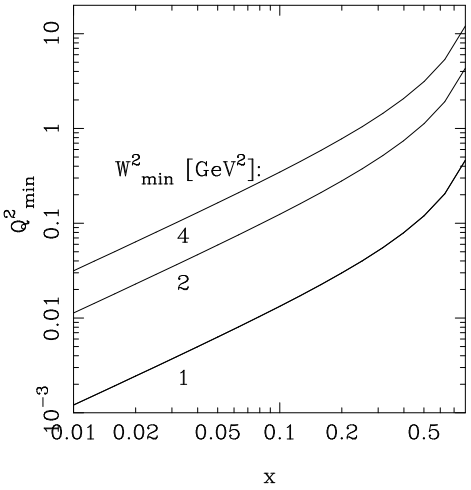

FIG. 1: Minimum value of Q^2 such that $W^2 > W^2_{\rm min} = 1,\ 2$ and 4 GeV^2.

and $x \equiv Q^2/(2p\cdot q)$. The nucleon mass is labeled with M. Kinematics show that the hadronic final state invariant mass is

$$W^2 = Q^2\left(\frac{1}{x} - 1\right) + M^2 \ , \tag{1}$$

so Q is kinematically allowed to range in the non-perturbative regime. Fig. 1 shows the minimum values of Q^2 such that $W^2 > W^2_{\rm min} = 1,\ 2$ and 4 GeV^2. The contribution of the low-Q^2 kinematic region to the DIS neutrino cross section is the focus of this paper.

The neutrino differential cross section can be written in terms of structure functions F_i as

$$\begin{aligned}\frac{d^2\sigma^{\nu}_{CC}(\nu N)}{dx\,dy} &= \frac{G_F^2 M E_\nu}{\pi(1+Q^2/M_W^2)^2}\left[xy^2F_1^{TMC}\right. \\ &+ \left(1 - y - \frac{Mxy}{2E_\nu}\right)F_2^{TMC} \\ &+ \left.\left(xy - \frac{xy^2}{2}\right)F_3^{TMC}\right] \end{aligned} \tag{2}$$

when the outgoing lepton mass is neglected. The full expression including lepton masses is found in Ref. [21], for example. Here, we assume ν_μ and $\bar\nu_\mu$ scattering and include the muon mass in our evaluation. The label of *TMC* indicates that target mass corrections can be incorporated into the structure functions [22, 23], both through the Nachtmann variable

$$\xi = \frac{2x}{Q^2(1+\rho)} \tag{3}$$

$$\rho = (1 + 4M_N^2x^2/Q^2)^{1/2} \ , \tag{4}$$

with nucleon mass dependent factors multiplying the asymptotic structure functions and with convolutions of the asymptotic structure functions.

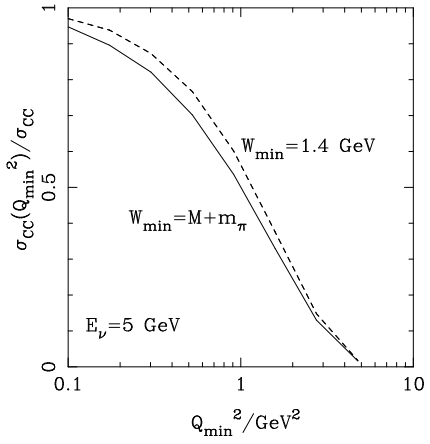

FIG. 2: $E_\nu = 5$ GeV including NLO QCD corrections and target mass corrections.

At leading order in QCD, neglecting target mass corrections and for values of Q large enough that the parton model makes sense, the structure functions are schematically

$$\begin{aligned} F_2(x,Q^2) &= 2xF_1(x,Q^2) \\ &= \sum 2x\big(q(x,Q^2) + \bar q(x,Q^2)\big) \\ F_3(x,Q^2) &= \sum 2\big(q(x,Q^2) - \bar q(x,Q^2)\big) \ . \end{aligned} \tag{5}$$

Only the relevant quarks and antiquarks are included above, and Cabibbo-Kobayashi-Maskawa mixing angles must be included as well. The full expressions, including NLO corrections, target mass corrections and charm mass corrections appear, e.g., in Ref. [20].

QCD corrections reduce the DIS cross section by about 10% for $E_\nu = 5 - 10$ GeV [20, 21]. The evaluation of the cross section at these energies relies on an extrapolation of the parton distribution functions to low Q. The parton distribution functions are typically not defined below a minimum factorization scale Q_0^2. We set the PDF scale at $Q^2 = Q_0^2$ for $Q^2 < Q_0^2$ and include the $O(\alpha_s)$ correction accounting for the mismatch of factorization scale with the scale Q. Fig. 2 shows the ratio of the charged current neutrino-nucleon cross section as a function of minimum Q^2 normalized to the total cross section for $E_\nu = 5$ GeV for two similar choices of $W^2_{\rm min} \sim 2$ GeV^2. Approximately half the cross section at this energy comes from $Q^2 < 1$ GeV^2. At higher energies, the fraction reduces, e.g. to $\sim 30\%$ at $E_\nu = 10$ GeV.

The importance of $Q^2 < 1$ GeV^2 in Fig. 2 leads us to consider structure functions at fixed values of Q for a range of x relevant to low energy neutrino scattering. We focus on F_2 at $Q^2 = 0.1,\ 0.5, 1$ and 4 GeV^2. At $Q^2 = 4$ GeV^2, we are firmly in the perturbative QCD regime, and at the low end of Q^2 we are definitely out of the perturbative regime. The range of x at fixed Q^2 is limited on the upper end by $W^2_{\rm min}$ as shown in Fig. 1. The lower limit on x is determined by the incident neutrino

energy: $x \geq Q^2/(2ME_\nu)$. Given the plethora of data in electromagnetic scattering, we turn to ep scattering to test the perturbative evaluation of the electromagnetic structure function F_2 and to consider alternatives.

III. ep SCATTERING

Electron-proton scattering in the perturbative regime is well described by the parton model. The structure function F_2 at leading order, neglecting target mass corrections, is written in terms of quark (and antiquark) distribution functions $q(x, Q^2)$ with electric charge $q = e_i e$:

$$F_2(x, Q^2) = \sum_i e_i^2 \Big(q(x, Q^2) + \bar{q}(x, Q^2) \Big) \ . \qquad (6)$$

As discussed above, the parton distribution functions are extrapolated below the minimum factorization scale Q_0^2 in the perturbative parton model evaluation.

Structure functions calculated in this manner can be compared with ep electromagnetic scattering data. For ease of comparison, we primarily use the parameterization of Abramowicz, Levin, Levy and Maor [11] which uses 23 parameters to describe a wide range of data. In Fig. 3 we show the ALLM parameterization (solid line), along with NLO QCD (dashed) evaluated using the Martin *et al.* parton distribution functions [24] MRST2004. The data points come from SLAC ep scattering data [25] for $Q^2 = 3.7 - 4.3$ GeV^2.

Also in shown in Fig. 3 are boxes indicating the relevant range of x for $Q^2 = 4$ GeV^2. The vertical line furthest left is $x_{\rm min}$ for $E_\nu = 10$ GeV, while the next vertical line is $x_{\rm min}$ for $E_\nu = 5$ GeV. The third vertical line shows $x_{\rm max}$ for $W^2_{\rm min} = 4$ GeV^2. At larger x is the maximum for $W^2_{\rm min} = 2$ GeV^2. The perturbative calculation matches the ALLM parameterization and the data well.

For comparison, we show the same curves for $Q^2 = 0.5$ GeV^2 along with data from E665 [26] in Fig. 4. The data are for $Q^2 = 0.43,\ 0.59$ GeV^2. The pertubative evaluation of F_2 overestimates the ALLM parameterization. On the basis of the discrepancy between ep data and the perturbative curves, we conclude that the low energy νN DIS cross section is overestimated by the perturbative expression.

Two other phenomenological parameterizations of electromagnetic structure functions are discussed here. The first is by Capella, Kaidalov, Merino and Thanh Van (CKMT) [16] and the second is the Bodek-Yang-Park parameterization [13, 14].

A. CKMT Parameterization

The CKMT parameterization [16] is based on the form

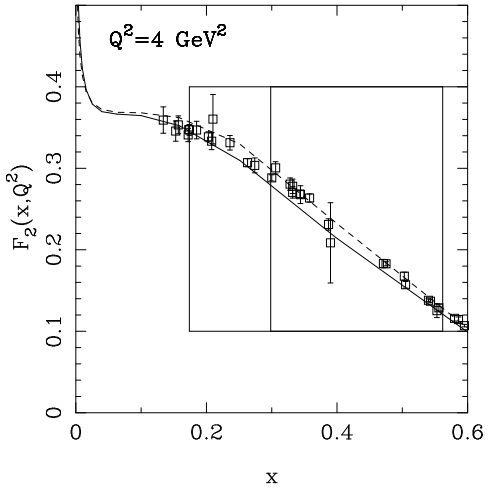

FIG. 3: $F_2(x, Q^2)$ for ep electromagnetic scattering for $Q^2 = 4$ GeV, with the ALLM parameterization (solid), NLO QCD (dashed) evaluated using the MRST2004. Also shown are representative data from Whitlow *et al.* [25] for $Q^2 = 3.7 - 4.3$ GeV^2.

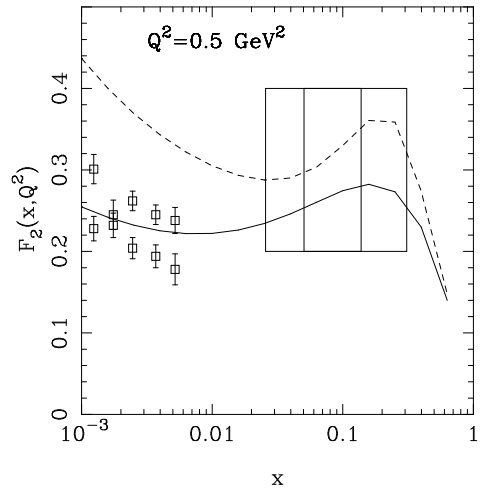

FIG. 4: $F_2(x, Q^2)$ for ep electromagnetic scattering for $Q^2 = 0.5$ GeV, with the ALLM parameterization (solid), NLO QCD (dashed). The data are from the E665 experiment [26] with $Q^2 = 0.43$ GeV^2 and 0.59 GeV^2.

$$\begin{aligned} F_2(x, Q^2) \ &= \ F_2^{sea}(x, Q^2) + F_2^{val}(x, Q^2) \\ &= \ Ax^{-\Delta(Q^2)}(1-x)^{n(Q^2)+4}\left(\frac{Q^2}{Q^2+a}\right)^{1+\Delta(Q^2)} \\ &+ \ Bx^{1-\alpha_R}(1-x)^{n(Q^2)}\left(\frac{Q^2}{Q^2+b}\right)^{\alpha_R} \\ &\times \ \Big(1 + f(1-x)\Big) \ . \qquad (7) \end{aligned}$$

The first term dominates at small x, where the physical picture is that photons fluctuate into $q\bar{q}$ pairs that form vector mesons. The second term dominates large x and is interpreted as the valence term. Characteristically, the

TABLE I: Parameter values in Ref. [13] for CKMT parameterization of the electromagnetic structure function F_2. The quantities B and f are determined from the valence conditions at $Q^2 = 2$ GeV^2 rather than fit.

Parameter	Value	Parameter	Value [GeV^2]
A	0.1502	a	0.2631
Δ_0	0.07684	d	1.1170
B	1.2064	b	0.6452
α_R	0.4250	c	3.5489
f	0.15		

valence d quark distribution has one extra power of $(1-x)$.

An interesting feature of this parameterization is its economy relative to the ALLM parameterization. The quantities B and f are calculated by requiring two valence u quarks and one valence d quark. This assumes that the first term (proportional to A) has no valence content. B is the coefficient of the up valence component, and f is the ratio of the down valence to up valence coefficients.

The quantities $n(Q^2)$ and $\Delta(Q^2)$ are parameterized by CKMT according to the form

$$n(Q^2) \;=\; \frac{3}{2}\left(1+\frac{Q^2}{Q^2+c}\right)\,, \tag{8}$$

$$\Delta(Q^2) \;=\; \Delta_0\left(1+\frac{2Q^2}{Q^2+d}\right)\,. \tag{9}$$

Values of the parameters from Ref. [16] appear in Table 1.

The quantity $\Delta_0 \simeq 0.08$ represents the power law of F_2 governed by pomeron exchange at low Q^2 [27]. This is the same power law that appears in the generalized vector meson dominance (GVDM) approach [28, 29]. The Q^2 dependent prefactor, however, has the same form as the continuum contribution rather than the vector meson contribution. Alwall and Ingelman [30] have taken the GVDM approach together with valence parton density functions based on a model accounting involving quantum fluctuations to consider ep scattering at low-Q^2. We take the more phenomenological CKMT approach to parameterizing F_2 in part because it is relatively straightforward to convert to νN structure functions.

A comparison of the ALLM parameterization and the CKMT parameterization of F_2 for electromagnetic scattering at $Q^2 = 0.1,\ 0.5, 1$ and 4 GeV^2 is shown in Fig. 5.

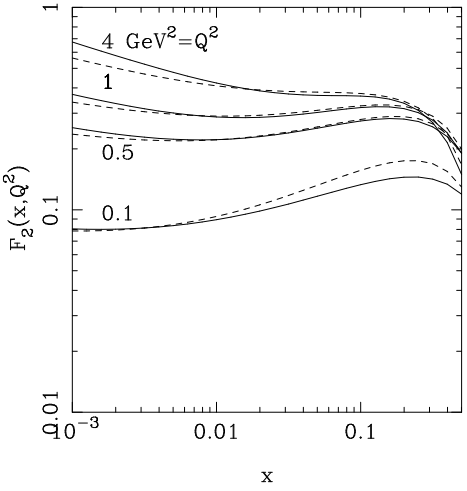

FIG. 5: $F_2(x, Q^2)$ for electromagnetic scattering with the ALLM parameterization (solid), and the CKMT parameterization (dashed).

B. Bodek-Yang-Park Parameterization

A second parameterization has been performed by Bodek and Yang [13], joined by Park [14]. A generalized Nachtman variable ξ_w is used, along with form factors and the Gluck, Reya and Vogt parton distribution functions (GRV98) [31]so that the structure function F_2 is written as

$$F_2(x,Q^2) \equiv \sum e_q^2 \xi_w (\tilde{q}(\xi_w,Q^2)\tilde{\bar{q}}(\xi_w,Q^2)\ . \tag{10}$$

The PDFs $\tilde{q}$ are related to the usual PDFs by form factor rescaling. Details are given in the appendix.

This approach is specifically designed to be used with neutrino scattering. One feature of the Bodek-Yang-Park (BYP) analysis is the separation of the quark and antiquark flavors. The flavor separated components of F_2 are then used to evaluate neutrino charged current interactions. To address the question of how universal the BYP parameterizations of effective quark distributions are, we will compare the BYP approach to evaluating the νN cross section with the CKMT parameterization. A comparison of these two cross section results will give an estimate of the uncertainty in the νN DIS cross section component. Ultimately, measurements in this kinematic regime are required.

IV. STRUCTURE FUNCTIONS IN NEUTRINO SCATTERING

The evaluation of the neutrino structure functions using the BYP parameterization are straightforward using

$$F_2(x,Q^2) \equiv \sum 2\xi_w (\tilde{q}(\xi_w,Q^2)\tilde{\bar{q}}(\xi_w,Q^2)\ . \tag{11}$$

The CKMT parameterization was fit specifically to ep scattering data, however, with the interpretation of the separate sea and valence terms, it can be modified to apply to neutrino scattering. Here we consider only isoscalar nucleons N, the average of proton plus neutron targets.

The modification of Eq. (7) will be done only for three parameters: A, B and f will be replaced by A_ν, B_ν and f_ν [17]. The rationale is that the small x and large x structure functions in electromagnetic and charged current scattering should show the same qualitative behavior as a function of Q^2. At large x, the balance between valence up and down quarks is different in electromagnetic and charged current scattering, however, the coefficients B and f are calculable. Qualitatively, for small-x, the structure functions are sea dominated. Again, the mix of sea components is changed, but the assumption is that each sea component has qualitatively the same behavior in x and Q^2, so only A changes.

One caveat to this approach is that at $Q^2 = 0$, PCAC requires a modification of the functional form of the parameterization [32]. Neither the BYP nor the CKMT parameterization currently accommodates this theoretical behavior. Nevertheless, the small x, small Q^2 data from neutrino scattering are accommodated. For example, the CCFR data [33] for $x = 0.008, 0.0125, 0.0175$ for $Q^2 = 0.4 - 0.9$ GeV^2 are within $\sim 10\%$ of the CKMT parameterization with neutrino modifications discussed below.

The modifications to Eq. (7) are the following. We calculate that for neutrino scattering $B \to B_\nu = 2.695$ and $f_\nu = 0.595$. By evaluating F_2 at $Q^2 = 10$ GeV^2, we choose $A \to A_\nu = 0.60$ so that it matches the NLO-TMC corrected F_2 reasonably well. This gives $A_\nu/A = 4$, which is what one would estimate by counting sea quarks and antiquarks contributing to each process, weighting s quarks and antiquarks by a factor of 1/2.

Fig. 6 shows a comparison of F_2 calculated using GRV98 PDFS at NLO in QCD with target mass corrections (solid line) and the Bodek-Yang-Park parameterization, both at $Q^2 = 4$ GeV^2. The two evaluations of F_2 agree well at this value of Q^2. At lower Q^2, the perturbative evaluation is larger than the BYP parameterization, for example, by about 30% at $x = 0.1$ and $Q^2 = 1$ GeV^2.

Fig. 7 shows the charged current F_2 using the modified CKMT (dashed lines) and the BYP (solid lines) parameterizations for several values of Q^2. The parameterizations give similar results except for the lowest value of Q^2 in the large x region, and for the smallest x values.

Cross sections require F_1 and F_3 as well as F_2. For the CKMT parameterization of F_3, we start with the valence term and add a strange quark component equal to 1/15 of the total sea contribution in F_2. To achieve a better large x agreement with perturbative QCD, the structure function has an overall normalization factor of 0.91. This factor makes the valence component integrate to 2.73 at $Q^2 = 2$ GeV^2, consistent with measurements [10] of the Gross-Llewellyn-Smith sum rule[35] including QCD corrections. To summarize, we take for neutrino scattering

$$F_3(x,Q^2) = \left[\frac{A_\nu}{15}x^{-\Delta(Q^2)}(1-x)^{n(Q^2)+4}\left(\frac{Q^2}{Q^2+a}\right)^{1+\Delta(Q^2)}\right.$$

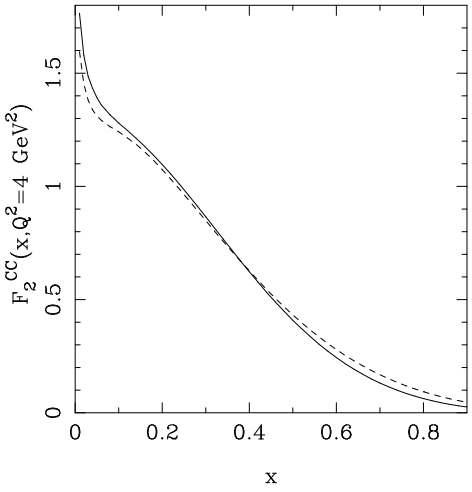

FIG. 6: Neutrino-isoscalar nucleon F_2 at $Q^2 = 4$ GeV^2 for charged current scattering, solid line for NLO QCD with TMC, dashed line from Bodek-Yang-Park parameterization using GRV98.

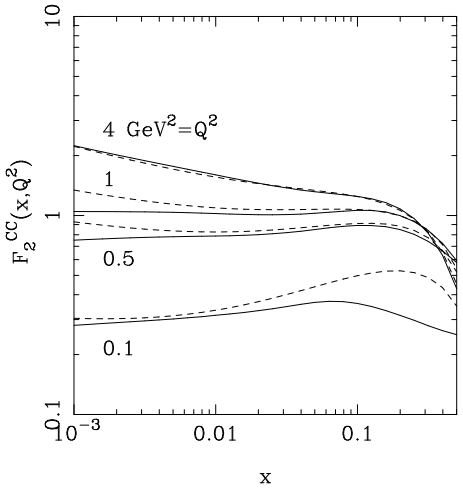

FIG. 7: Neutrino-isoscalar nucleon F_2 at $Q^2 = 0.1$, 0.5, 1 and 4 GeV^2 for charged current scattering, solid line for the Bodek-Yang-Park parameterization using GRV98 and the dashed line for the modified CKMT parameterization with $A_\nu = 0.60$, $B_\nu = 2.695$ and $f = 0.595$.

$$+ \left. B_\nu x^{1-\alpha_R}(1-x)^{n(Q^2)}\left(\frac{Q^2}{Q^2+b}\right)^{\alpha_R}\right.$$
$$\times \left.\Big(1+f_\nu(1-x)\Big)\right]/(1.1x)\ . \qquad (12)$$

F_1 is obtained from F_2 by including the correction for $R \neq 0$ where

$$R = \frac{F_2}{2xF_1}\left(1+\frac{4M^2x^2}{Q^2}\right) - 1\ . \qquad (13)$$

We use the parameterization of Whitlow et al. in

Ref. [25], which is also consistent with neutrino scattering data [36]. The parameterization applies for $Q^2 > Q^2_m = 0.3$ GeV^2. Below $Q^2 = Q^2_m$, we take $R(x,Q^2) = R(x,Q^2_m) \cdot Q^2/Q^2_m$.

We note that similar results for the structure functions are obtained by rescaling the NLO+TMC in a manner similar to Eq. (7), e.g., below the scale Q^2_c,

$$\bar{u}(\xi,Q^2) = \bar{u}(\xi,Q^2_c) \cdot F_2^{sea}(x,Q^2)/F_2^{sea}(x,Q^2_c) \qquad (14)$$

and similarly for the valence distributions. The gluon distribution must be rescaled according to the "sea" factor.

V. NEUTRINO-NUCLEON CROSS SECTION

The neutrino cross section with isoscalar nucleon targets is calculated using Eq. (2). For the results labeled by the low-Q^2 parameterization, we use the full NLO QCD corrected structure functions including target mass corrections for $Q^2 > Q^2_c = 4$ GeV^2. Below Q^2_c, we use either the BYP or CKMT parameterizations of the nonperturbative region. For the energies considered here, below 10 GeV, the results are not very sensitive to the cutoff Q_c. At the lowest energies, the nonperturbative parameterization is relatively more important, however, the cross sections are small.

Results labeled with NLO+TMC, as in previous sections, used the next-to-leading order QCD corrected structure functions, with parton distribution functions frozen at the minimum value provided by the parameterization. For this section, all NLO+TMC results used the GRV98 PDFs with a minimum $Q^2 = 0.8$ GeV^2.

In Fig. 8 we show the neutrino-nucleon charged current cross section normalized by incident neutrino energy, where the cross section have been evaluated using NLO+TMC (upper lines) and using the CKMT and BYP parameterizations below $Q^2_c = 4$ GeV^2 (lower lines) for $W^2_{\rm min} = 4$ GeV^2 (solid) and 2 GeV^2 (dashed). The dotted lines show the cross sections calculated using leading order QCD including target mass correction. Numerical values corresponding to this figure are shown in Table II. The corresponding results for antineutrino-nucleon scattering are shown in Fig. 9 and Table III.

The low Q^2 corrections reduce the cross sections even at $E_\nu = 10$ GeV. For $W^2_{\rm min} = 2$ GeV^2 for neutrinos, the reduction is by 7-8% at 10 GeV, and 11-13% at 5 GeV. For neutrino scattering with $W^2_{\rm min} = 4$ GeV^2 the reduction ranges from 6-7% to 10-15% for the same energies. Antineutrino scattering cross sections are more dramatically affected. The cross sections are reduced by of order 20% for $E_{\bar{\nu}} = 10$ GeV, and between 25-43% depending on $W^2_{\rm min}$ for 5 GeV incident antineutrinos. The sensitivity to the value of Q^2_c is greater, a few percent, at $E_{\bar{\nu}} = 10$ GeV.

The agreement between the cross sections calculated with the CKMT and BYP parameterizations gives some confidence in the predictions for the DIS component of the neutrino-nucleon cross section at a few GeV in energy. This is one step in developing the comprehensive calculation of the neutrino cross section required for interpreting the oscillation measurements at present and in the future.

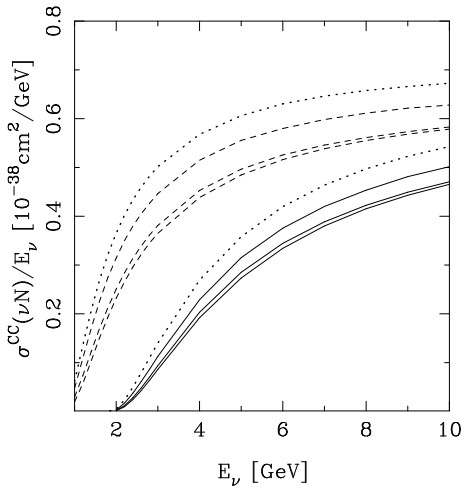

FIG. 8: Neutrino-isoscalar nucleon cross sections normalized to incident neutrino energy: solid lines for $W^2_{\rm min} = 4$ GeV^2 and dashed lines for $W^2_{\rm min} = 2$ GeV^2. The upper solid and dashed lines use NLO QCD plus target mass corrections to evaluate the cross section, while the lower solid and dashed lines use the CKMT and BYP parameterizations below $Q^2 = 4$ GeV^2. The dotted lines show the evaluation using leading order QCD plus target mass corrections.

Appendix

The form of the Bodek-Yang-Park parameterization [13, 14] used in this paper relies on parameterizations of the form

$$F_2(x,Q^2) \equiv \sum e_q^2 \xi_w \tilde{q}(\xi_w,Q^2) \qquad (15)$$

where $\tilde{q}(\xi_w,Q^2)$ depends on rescaled Gluck, Reya and Vogt PDFs [31] in terms of a modified Nachtman variable ξ_w. For massless final state quarks ξ_w is used, while for charm production, ξ_{wc} is used instead. They are defined as

$$\begin{aligned}
\xi_w &= \frac{2x(Q^2+B)}{Q^2(1+\rho)+2Ax} \\
\xi_{wc} &= \frac{2x(Q^2+B+m_c^2)}{Q^2(1+\rho)+2Ax} \\
A &= 0.538 \text{ GeV}^2 \\
B &= 0.305 \text{ GeV}^2 \\
m_c &= 1.5 \text{ GeV} \\
\rho &= (1+4M_N^2x^2/Q^2)^{1/2}
\end{aligned}$$

E_ν [GeV]	NLO+TMC $W^2_{\rm min} = 2$ GeV^2	BYP	CKMT	NLO+TMC $W^2_{\rm min} = 4$ GeV^2	BYP	CKMT
1	4.77e-2	1.96e-2	2.93e-2			
2	6.29e-1	4.64e-1	5.02e-1	6.40e-3	2.83e-3	4.08e-3
3	1.34	1.10	1.14	3.38e-1	2.58e-1	2.81e-1
5	2.78	2.42	2.48	1.56	1.37	1.43
10	6.28	5.78	5.83	5.02	4.65	4.71

TABLE II: Neutrino-nucleon charged current cross section, in units of 10^{-38} cm^2, calculated using NLO QCD with target mass corrections, with the Bodek-Yang-Park parameterization and with the Capella et al. parameterization below $Q^2_0 = 4$ GeV^2.

$E_{\bar\nu}$ [GeV]	NLO+TMC $W^2_{\rm min} = 2$ GeV^2	BYP	CKMT	NLO+TMC $W^2_{\rm min} = 4$ GeV^2	BYP	CKMT
1	1.49e-2	2.17e-3	1.71e-3			
2	1.93e-1	6.79e-2	9.58e-2	2.64e-3	4.43e-4	2.22e-4
3	4.55e-1	2.27e-1	2.92e-1	9.29e-2	3.29e-2	3.45e-2
5	1.06	6.89e-1	7.87e-1	4.46e-1	2.56e-1	2.99e-1
10	2.70	2.11	2.19	1.78	1.38	1.43

TABLE III: Antineutrino-nucleon charged current cross section, in units of 10^{-38} cm^2, calculated using NLO QCD with target mass corrections, with the Bodek-Yang-Park parameterization and with the Capella et al. parameterization below $Q^2_0 = 4$ GeV^2.

The rescaling of the PDFs is of the form

$$\begin{aligned}
\tilde{u}_v &= \frac{(1-G_D^2)\cdot(Q^2+C_{2vu})}{Q^2+C_{1vu}}u_v \\
\tilde{d}_v &= \frac{(1-G_D^2)\cdot(Q^2+C_{2vd})}{Q^2+C_{1vd}}d_v \\
\tilde{\bar{u}} &= \frac{Q^2}{Q^2+C_{su}}\bar{u} \text{ (and sim. for } \tilde{\bar{d}}, \tilde{\bar{s}})
\end{aligned}$$

where $G_D = (1 + Q^2/(0.71\ \text{GeV}^2))^{-2}$. The valence and sea K factors are:

$$\begin{aligned}
C_{1vu} &= 0.291\ \text{GeV}^2 \qquad C_{1vd} = 0.202\ \text{GeV}^2 \\
C_{2vu} &= 0.189\ \text{GeV}^2 \qquad C_{2vd} = 0.255\ \text{GeV}^2 \\
C_{su} &= 0.363\ \text{GeV}^2 \qquad C_{sd} = 0.621\ \text{GeV}^2 \\
C_{ss} &= 0.380\ \text{GeV}^2\ .
\end{aligned}$$

Acknowledgments

This work was supported in part by DOE Contract DE-FG02-91ER40664. The author thanks Y. Meurice, I. Sarcevic and especially S. Kretzer for contributions and comments.

[1] For a review, see, e.g., M. Maltoni, T. Schwetz, M. A. Tortola and J. W. F. Valle, New J. Phys. **6**, 122 (2004).

[2] S. Fukuda *et al.* [Super-Kamiokande Collaboration], Phys. Lett. B **539**, 179 (2002), Q. R. Ahmad *et al.* [SNO Collaboration], Phys. Rev. Lett. **89**, 011301 (2002).

[3] Y. Fukuda *et al.* [Super-Kamiokande Collaboration], Phys. Rev. Lett. **81**, 1562 (1998).

[4] M. H. Ahn *et al.* [K2K Collaboration], Phys. Rev. Lett. **90**, 041801 (2003). P. Adamson *et al.* [MINOS Collaboration], arXiv:hep-ex/0512036.

[5] P. Lipari, M. Lusignoli and F. Sartogo, Phys. Rev. Lett. **74**, 4384 (1995).

[6] G. P. Zeller, arXiv:hep-ex/0312061.

[7] K. S. McFarland, Eur. Phys. J. A **24S2**, 187 (2005) and http://minerva.fnal.gov/.

[8] S. Brice *et al.*, Nucl. Phys. Proc. Suppl. **139**, 317 (2005) and http://www-finesse.fnal.gov/.

[9] K. S. Kuzmin, V. V. Lyubushkin and V. A. Naumov, arXiv:hep-ph/0511308.

[10] S. Eidelman *et al.* [Particle Data Group], Phys. Lett. B **592**, 1 (2004).

[11] H. Abramowicz, E. M. Levin, A. Levy and U. Maor, Phys. Lett. B **269**, 465 (1991). H. Abramowicz and A. Levy, arXiv:hep-ph/9712415.

[12] See, e.g., P. Desgrolard and E. Martynov, Eur. Phys. J. C **22**, 479 (2001), A. Donnachie and P. V. Landshoff, Phys. Lett. B **518**, 63 (2001).

[13] U. K. Yang and A. Bodek, Phys. Rev. Lett. **82**, 2467 (1999); A. Bodek and U. K. Yang, arXiv:hep-ex/0308007.

[14] A. Bodek, I. Park and U. k. Yang, Nucl. Phys. Proc. Suppl. **139**, 113 (2005).

[15] See also, S. A. Kulagin and R. Petti, Nucl. Phys. A **765**, 126 (2006).

[16] A. Capella, A. Kaidalov, C. Merino and J. Tran Thanh Van Phys. Lett. B **337**, 358 (1994).

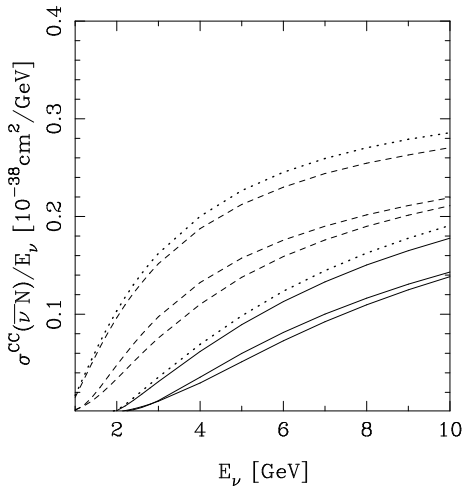

FIG. 9: Anti-neutrino-isoscalar nucleon cross sections normalized to incident anti-neutrino energy: solid lines for $W^2_{\rm min} = 4$ GeV^2 and dashed lines for $W^2_{\rm min} = 2$ GeV^2. The upper solid and dashed lines use NLO QCD plus target mass corrections to evaluate the cross section, while the lower solid and dashed lines use the CKMT and BYP parameterizations below $Q^2 = 4$ GeV^2. The dotted lines show the evaluation using leading order QCD plus target mass corrections.

[17] A. Capella, A. Kaidalov, C. Merino and J. Tran Thanh Van, *Proceedings of 29th Rencontres de Moriond: QCD and High-energy Hadronic Interactions, Meribel les Allues, France, 19-26 Mar 1994*, pp. 271-282.

[18] C. H. Llewellyn Smith, Phys. Rept. **3**, 261 (1972); see J. Monroe [MiniBooNE Collaboration], Nucl. Phys. Proc. Suppl. **139**, 59 (2005) for recent measurements.

[19] D. Rein and L. M. Sehgal, Nucl. Phys. B **223**, 29 (1983); G. L. Fogli and G. Nardulli, Nucl. Phys. B **160**, 116 (1979); E. A. Paschos, J. Y. Yu and M. Sakuda, Phys. Rev. D **69**, 014013 (2004); E. A. Paschos, L. Pasquali and J. Y. Yu, Nucl. Phys. B **588**, 263 (2000).

[20] See, e.g., S. Kretzer and M. H. Reno, Phys. Rev. D **69**, 034002 (2004), Phys. Rev. D **66**, 113007 (2002) and references therein.

[21] S. Kretzer and M. H. Reno, Nucl. Phys. Proc. Suppl. **139**, 134 (2005).

[22] H. Georgi and H. D. Politzer, Phys. Rev. D **14**, 1829 (1976); A. De Rujula, H. Georgi and H. D. Politzer, Annals Phys. **103**, 315 (1977).

[23] R. Barbieri, J. R. Ellis, M. K. Gaillard and G. G. Ross, Nucl. Phys. B **117**, 50 (1976).

[24] A. D. Martin, R. G. Roberts, W. J. Stirling and R. S. Thorne, Phys. Lett. B **604**, 61 (2004).

[25] L. W. Whitlow, S. Rock, A. Bodek, E. M. Riordan, S. Dasu, Phys. Lett. B **250**, 193 (1990).

[26] M. R. Adams *et al.* [E665 Collaboration], Phys. Rev. D **54**, 3006 (1996).

[27] A. Donnachie and P. V. Landshoff, Phys. Lett. B **296**, 227 (1992).

[28] J. J. Sakurai and D. Schildknecht, Phys. Lett. B **40** (1972) 121.

[29] B. Badelek and J. Kwiecinski, Phys. Lett. B **295**, 263 (1992); B. Badelek and J. Kwiecinski, Rev. Mod. Phys. **68**, 445 (1996).

[30] J. Alwall and G. Ingelman, Phys. Lett. B **596**, 77 (2004), J. Alwall and G. Ingelman, Phys. Rev. D **71**, 094015 (2005).

[31] M. Gluck, E. Reya and A. Vogt, Eur. Phys. J. C **5**, 461 (1998).

[32] S. L. Adler, Phys. Rev. **135**, B964 (1964).

[33] B. T. Fleming *et al.* [CCFR Collaboration], Phys. Rev. Lett. **86**, 5430 (2001), B. T. Fleming, FERMILAB-THESIS-2001-02

[34] J. Pumplin, D. R. Stump, J. Huston, H. L. Lai, P. Nadolsky and W. K. Tung, JHEP **0207**, 012 (2002).

[35] D. Gross and C. H. Llewellyn Smith, Nucl. Phys. B **14**, 337 (1969).

[36] G. Onenugut et al., CHORUS Collaboration, Phys. Lett. B **632**, 65 (2006).